

# Supervised Learning of Functional Maps for Infarct Classification

Anirban Mukhopadhyay<sup>1</sup>, Ilkay Oksuz<sup>2</sup>(✉), and Sotirios A. Tsaftaris<sup>2,3</sup>

<sup>1</sup> Zuse Institute Berlin, Berlin, Germany

<sup>2</sup> IMT Institute for Advanced Studies Lucca, Lucca, Italy

`ilkay.oksuz@imtlucca.it`

<sup>3</sup> Department of Electrical Engineering and Computer Science,  
Northwestern University, Evanston, USA

**Abstract.** Our submission to the STACOM Challenge at MICCAI 2015 is based on the supervised learning of functional map representation between End Systole (ES) and End Diastole (ED) phases of Left Ventricle (LV), for classifying infarcted LV from the healthy ones. The Laplace-Beltrami eigen-spectrum of the LV surfaces at ES and ED, represented by their triangular meshes, are used to compute the functional maps. Multi-scale distortions induced by the mapping, are further calculated by singular value decomposition of the functional map. During training, the information of whether an LV surface is healthy or diseased is known, and this information is used to train an SVM classifier for the singular values at multiple scales corresponding to the distorted areas augmented with surface area difference of epicardium and endocardium meshes. At testing similar augmented features are calculated and fed to the SVM model for classification. Promising results are obtained on both cross validation of training data as well as on testing data, which encourages us in believing that this algorithm will perform favourably in comparison to state of the art methods.

**Keywords:** Infarct · Cardiac remodeling · Laplace-Beltrami · SVM · SVD

## 1 Introduction

Cardiac remodeling is a clinical term to refer the geometric changes occur on the Left Ventricle (LV) due to myocardial infarction. This phenomenon is considered as an important predictor for survival [14] in clinical practice. However current clinical practices are limited to simple quantities like mass, volume, dimension ratio etc. for important predictions. As a result, important geometric quantities are completely ignored in clinical practice, and only few recent studies on small population have been proposed to quantitatively measure the geometrical structural modification of LV during cardiac remodeling in Multirow Detector Computer Tomography (MDCT) images [8–10].

However, large population-based studies have been recently performed using cardiovascular magnetic resonance (CMR) imaging [2]. CMR, as a non-invasive radiation-free modality, provides rich and detailed quantitative data of the cardiac function and structure. The main goal of the STACOM 2015 challenge is to employ shape analysis and pattern recognition techniques to quantitatively measure geometric changes during cardiac remodeling. In this paper, rather than approaching the problem in a pure feature-driven binary classification technique, we aimed quantifying and visualizing the shape deformation between End Systolic (ES) and End Diastolic (ED) states for healthy and diseased LVs.

Cardiac remodeling results in contraction of myocardium and volume. When represented as a 2D manifold embedded in 3D space, these quantities can be approximated by the surface area of the 2D manifold discretized as a triangular mesh. As a result, a measure of surface area distortion can effectively quantify cardiac remodeling. Moreover, we have also observed that the area distortion of LV is a multi-scale phenomenon and tried to model it in a similar multi-scale fashion (from global to local) to emphasize actual physiological changes. In terms of machine learning, these steps can be considered as a feature selection procedure which ensures the selection of most distinguishing features. In particular, we have incorporated the recently developed functional map framework [11,12] to analyze and visualize ES-ED shape variation between healthy and diseased LVs.

We hypothesize that by learning the features of those regions, where the ES-ED deformation has introduced maximum distortion, we can successfully quantify the geometric changes during cardiac remodeling. The main contributions of this paper are twofold. First, we introduce Functional Map based shape variation exploration in cardiac image analysis context. Second, we present supervised learning of localized feature variations for quantifying cardiac remodeling. The remainder of the paper is organized as follows: Sect. 2 discusses related work, Sect. 3 presents the proposed method, whereas the implementation details are described in Sect. 4. Results are described in Sect. 5 and finally, Sect. 6 offers discussions and conclusion.

## 2 Related Work

Finite-element analysis has been the de-facto standard for modeling LV shape and function, providing measures accurate enough to be incorporated into clinical practice [7]. Principal component analysis (PCA) is extensively used for analyzing the modes of shape patterns found in populations [1]. However, the unsupervised nature of PCA is sometimes limited towards finding clinically interpretable features.

The most advanced technique for quantifying geometric changes during cardiac remodeling is proposed by Mukhopadhyay et al. in this series of work [8–10]. Here, the authors have proposed 3D Bag-of-words approach with extrinsic and intrinsic isometry invariant geometric features for quantifying local cardiac remodeling. However, this work does not address the multi-scale properties of distortion introduced by cardiac remodeling.

### 3 Method

In the proposed approach, we have relied on derived quantities of functional maps, in order to learn the distortions introduced during cardiac remodeling. Before describing the proposed approach in detail, we provided an overview of the functional map framework proposed by Ovsjanikov et al. [11] in Sect. 3.1 and the distortion analysis mechanism [12] in Sect. 3.2.

#### 3.1 Functional Maps

A functional map is a novel approach for inference and manipulation of maps between shapes that tries to resolve the issues of correspondences in a fundamentally different manner. Rather than plotting the corresponding points on the shapes, the mappings between functions defined on the shapes are considered. This notion of correspondence generalizes the standard point-to-point map since every point-wise correspondence induces a mapping between function spaces, while the opposite, in general, is not true.

The proposed functional map framework described above provides an elegant way, using a functional representation, to avoid direct representation of correspondences as mappings between shapes. Ovsjanikov et al. [11] have noted that when two shapes  $X$  and  $Y$  are related by a bijective correspondence  $t : X \rightarrow Y$  and endowed with measures  $\mu_X$  and  $\mu_Y$ , then for any real function  $f : X \rightarrow \mathbb{R}$ , one can construct a corresponding function  $g : Y \rightarrow \mathbb{R}$  as  $g : f \circ t^{-1}$ . In other words, the correspondence  $t$  uniquely defines a mapping between the two function spaces  $F(X, \mathbb{R}) \rightarrow F(Y, \mathbb{R})$ , where  $F(X, \mathbb{R})$  denotes the space of real functions on  $X$ . Equipping  $X$  and  $Y$  with harmonic bases,  $\{\phi_i\}_{i \geq 1}$  and  $\{\psi_j\}_{j \geq 1}$ , respectively, one can represent a function  $f : X \rightarrow \mathbb{R}$  using the set of (generalized) Fourier coefficients  $\{a_i\}_{i \geq 1}$  as  $f = \sum_{i \geq 1} a_i \phi_i$ .

Translating this representation into the other harmonic basis  $\{\psi_j\}_{j \geq 1}$ , one obtains a simple representation of the correspondence between the shapes given by  $T(f) = \sum_{i,j \geq 1} a_i c_{ij} \psi_j$  where  $c_{ij}$  are Fourier coefficients of the basis functions of  $X$  expressed in the basis of  $Y$ , defined as  $T(\phi_i) = \sum_{j \geq 1} c_{ij} \psi_j$ . The correspondence  $t$  between the shapes can thus be approximated using  $k$  basis functions and encoded using a  $k \times k$  matrix  $C = (c_{ij})$  of these Fourier coefficients, referred to as the functional matrix. In this representation, the computation of the shape correspondence  $t : X \rightarrow Y$  is translated into a simpler task of determining the functional matrix  $C$  from a set of correspondence constraints. The matrix  $C$  has a diagonal structure if the harmonic bases  $\{\phi_i\}_{i \geq 1}$  and  $\{\psi_j\}_{j \geq 1}$  are compatible, which is a crucial property for the efficient computation of the correspondence.

#### 3.2 Analyzing Functional Maps

Here, the main goal is to isolate the regions where the map has induced significant distortion at various scales. This is simply achieved by considering the functional representation of a map  $C$  and performing spectral analysis on this representation, as shown in Figs. 1 and 2. It is expected that for an optimal map

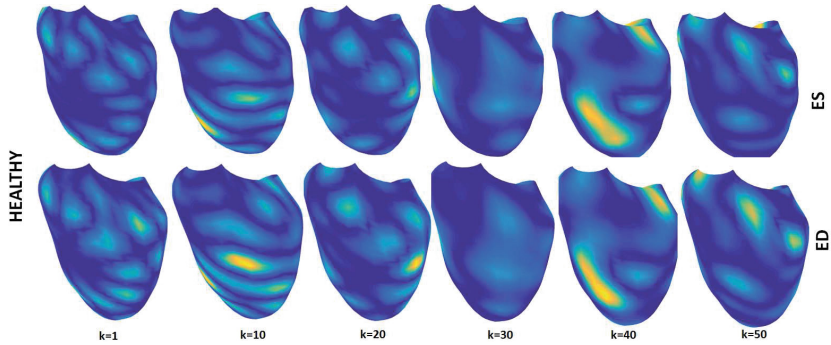


**Fig. 1.** The region where the map has distorted the area measure the most, at various scales  $k$  for an exemplary healthy subject. Note that the region is becoming more and more local with increasing values of  $k$ .

$t : X \rightarrow Y$ ,  $\mu_X$  and  $\mu_Y$  should be preserved. For the analysis and visualization of the distortion, Ovsjanikov et al. [12] and Rustomov et al. [13] proposed to use a real valued function  $w : Y \rightarrow \mathbb{R}$  which will be used for mapping distortions on  $Y$  and  $w \circ t$  for  $X$ . We have chosen area-distortion similar to [13] as the preferred measure of distortion.

It is proved in [12], that the optimal  $w$  can be derived by  $w_k^* = \phi_{1\dots k}^N w$  where  $\phi_{1\dots k}^N$  contains the first  $k$  eigenfunctions of the surface Laplacian operator and  $w$  is the right singular vector corresponding to the largest singular value of  $C$ . In addition, the scalars  $S_k$  has the ability to quantify the distortion at the various scales  $k$ . It is interesting to note that this technique does not place any assumptions on the geometry or topology of the function  $w$ , but provides a scale parameter  $k$ , which is more intuitive for understanding the scales of distortion. Large values of  $k$  allow for highly localized distortions, whereas medium and small values of  $k$  enforce the indicator functions to be more smooth resulting in the determination of globally problematic regions. In particular, the singular values  $C$  associated with each singular vector, indicates the amount of distortion introduced by the map at that particular scale.

### 3.3 Supervised Learning of Shape Distortions

We propose to learn the areas where the map has induced significant distortion between the End Systole and the End Diastole phases of a healthy versus diseased subject. In particular, we have achieved this by learning singular values associated with distortions at multiple scales concatenated with the difference of overall surface area of endo and epicardium at ES and ED. We subtracted the total area of endocardium at ED from the total area of endocardium at ES. We repeated the same operation for epicardium and used both features. We have chosen the vector of singular values  $c_k \in C$  as the feature vector representing the distortion between ES and ED. The STACOM 2015 dataset contains labeled

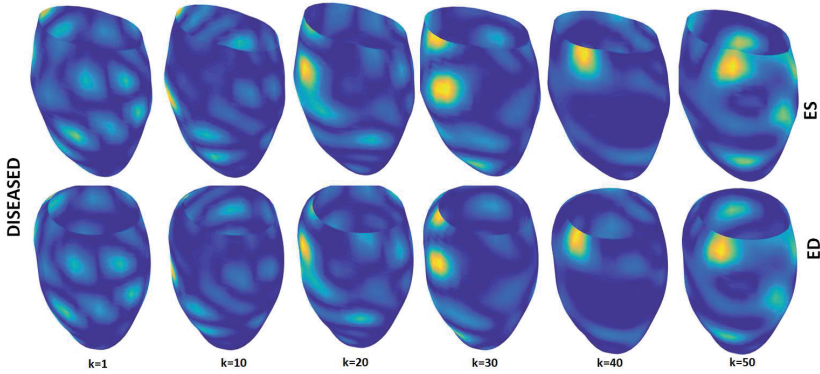


**Fig. 2.** The region where the map has distorted the area measure the most, at various scales  $k$  for an exemplary diseased subject.

dataset of 100 healthy and 100 diseased subjects, which is used for training a decision boundary of Support Vector Machine (SVM). During testing, similar feature selection procedure is used, followed by evaluation using the learnt decision boundary to consider whether the given meshes are from a normal subject or from a diseased one.

## 4 Implementation

We have employed a two step strategy for practical implementation of the problem, due to computational complexity of the method described in Sect. 3. In particular, we have adopted a Active Shape Model (ASM) [4] to resolve the relatively easier test cases. Eight different ASMs are trained on training datasets, four for normal and four for diseased cases. For either normal or diseased case, one ASM is trained for ES epi and endocardium, as well as ED epi and endocardium. For the test cases, the representative class of each surface is determined by finding the lower  $L_2$  error across all points. The first screening of test cases results in determination of a class if 3 of the 4 shapes agree to a common class. Otherwise the test case is evaluated using the method described in Sect. 3.

We have used the *Mesh Laplacian* implementation of [15], for computing the basis functions. These basis functions are used for the functional map calculation and analysis. It is important to note that because of the orthonormality of our chosen basis, matrix of area-based inner product reduces to the identity matrix. Surface area of LV endo and epicardium meshes are calculated using the implementation of [6]. The supervised learning using SVM is performed using the *libSVM* implementation of Chang et al. [3]. In particular we have chosen a polynomial kernel of the following form  $(\gamma u'v + c)^d$ , where  $\gamma = 2$ ,  $c = 2$  and  $d = 5$ .

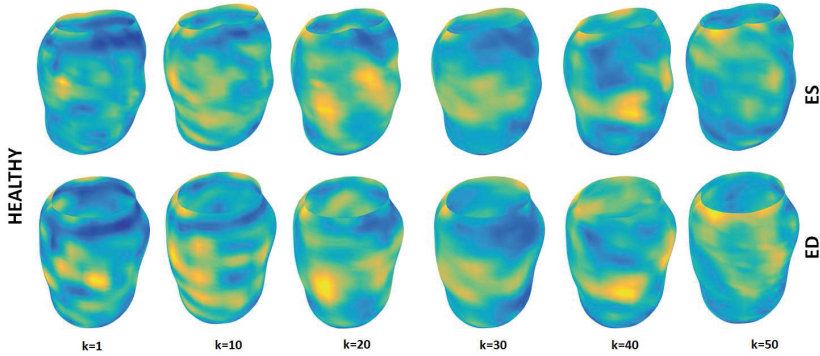


**Fig. 3.** The region where the map has distorted the area measure the most over the whole population of healthy subjects from STACOM 2015 training dataset, at various scales  $k$ .

## 5 Results

### 5.1 Data

Here we use the data available through the STACOM 2015 challenge for modeling the statistical shape of the left ventricle (LV). The STACOM training dataset contains 100 cases with myocardial infarction and another 100 healthy cases. The myocardial infarction cases are acquired through DETERMINE and the healthy ones through MESA [5]. In particular, the MESA study protocol ensured that these subjects did not have physician-diagnosed heart attack, angina, stroke, heart failure or atrial fibrillation, or undergone procedures related to cardiovascular disease. The testing set contains another set of 100 healthy and 100 diseased cases, for which the disease status is unknown to us and is evaluated by the co-organizers.

### 5.2 Qualitative Evaluation

To evaluate our preliminary results qualitatively, we have chosen to visualize the multi-scale distortion measure between ES and ED phases of a randomly sampled healthy and diseased subject as shown in Figs. 1 and 2. Since this yielded promising results, as evidenced from the multi-scale nature of the distortion, we have tried to further characterize population-level distortions between ES and ED phase of healthy and diseased subjects. In Figs. 3 and 4, population-level multiscale distortions of healthy and diseased subject respectively, are projected on two exemplary surfaces to visualize the differences. Different patterns of distortion is quite evident from Figs. 3 and 4, which motivates us for further quantitative analysis using machine learning techniques and check the accuracy of the proposed method in the STACOM 2015 challenge.

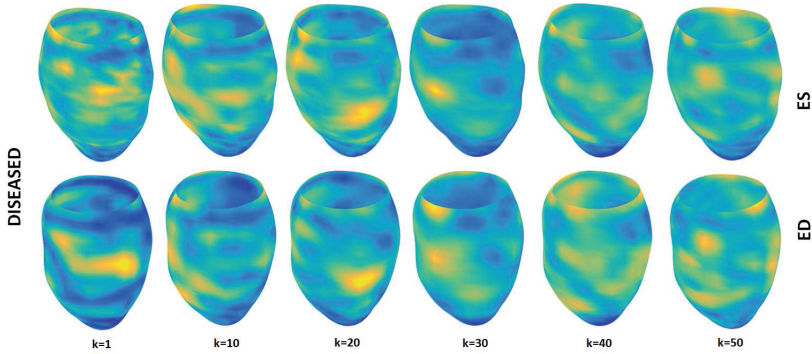


**Fig. 4.** The region where the map has distorted the area measure the most over the whole population of diseased subjects from STACOM 2015 training dataset, at various scales  $k$ .

### 5.3 Quantitative Evaluation

We have evaluated our algorithm on the training data set to estimate the performance. We have used a 10-fold cross-validation to evaluate the performance of the method and we have reached an average accuracy of 95.67 and a standard deviation of 1.26.

Furthermore, we have built a set-up to estimate the effect of number of training subjects on the accuracy. Figure 5 shows the influence of varying the total number of training subjects  $n$ , equally divided between normal and diseased cases, from  $n = 20$  to  $n = 180$  with the rest as testing subjects. The training samples are sampled randomly and for each  $n$ , we have run 50 experiments and reported the mean accuracy. It can be observed that increasing number of training subjects enable the algorithm to reach higher training accuracy.

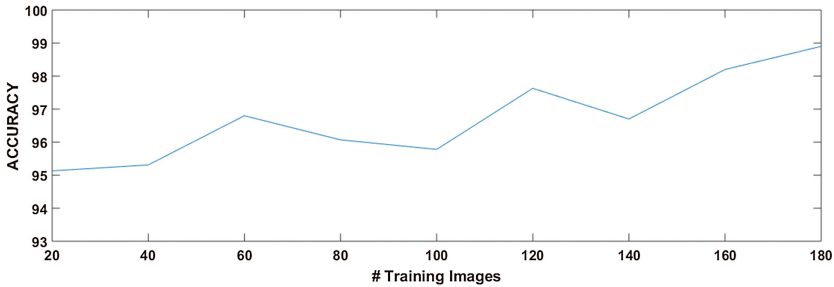


**Fig. 5.** The influence of the number of training subjects on accuracy

## 6 Discussions and Conclusion

Myocardial infarction results in a significant change of LV geometry due to the cardiac remodeling phenomenon. In this paper, we have proposed a framework to effectively differentiate the distortion between ES and ED phase of a healthy LV and diseased LV. Our proposed multi-scale approach is capable of describing distortions from global to local scale, which we have exploited in a supervised learning framework for the STACOM 2015 challenge. The preliminary visualizations and quantitative results suggest a population-wide common distortion pattern for healthy LVs, which can be utilized further in larger clinical studies. In this work, we have not considered the clinical quantities for describing cardiac remodeling such as Wall Thickness, Conicity, Sphericity etc. In the future, these quantities can be easily incorporated into the feature vector, to enhance the quantitative performance. Finally, the quantification of the distortion using singular values enable the possibility to extend this method for longitudinal studies of diseased LVs, and quantification of distortion over time.

## References

1. Augenstein, K.F., et al.: Finite element modeling for three-dimensional motion reconstruction and analysis. In: Amini, A.A., Prince, J.L. (eds.) MCDM. Computational Imaging and Vision, vol. 23, pp. 37–58. Springer, The Netherlands (2001)
2. Bild, D.E., et al.: Multi-ethnic study of atherosclerosis: objectives and design. *AJE* **156**(9), 871–881 (2002)
3. Chang, C.C., et al.: LIBSVM: a library for support vector machines. *TIST* **2**(3), 27 (2011)
4. Cootes, T.F., et al.: Active shape models - their training and application. *CVIU* **61**(1), 38–59 (1995)
5. Fonseca, C.G., et al.: The cardiac atlas project—an imaging database for computational modeling and statistical atlases of the heart. *Bioinformatics* **27**(16), 2288–2295 (2011)
6. Legland, D.: Geom3d Toolbox. <http://de.mathworks.com/matlabcentral/fileexchange/24484-geom3d>
7. Li, B., et al.: In-line automated tracking for ventricular function with magnetic resonance imaging. *JACC* **3**(8), 860–866 (2010)
8. Mukhopadhyay, A., Qian, Z., Bhandarkar, S., Liu, T., Voros, S.: Shape analysis of the left ventricular endocardial surface and its application in detecting coronary artery disease. In: Metaxas, D.N., Axel, L. (eds.) FIMH 2011. LNCS, vol. 6666, pp. 275–283. Springer, Heidelberg (2011)
9. Mukhopadhyay, A., Qian, Z., Bhandarkar, S.M., Liu, T., Rinehart, S., Voros, S.: Morphological analysis of the left ventricular endocardial surface and its clinical implications. In: Ayache, N., Delingette, H., Golland, P., Mori, K. (eds.) MICCAI 2012, Part II. LNCS, vol. 7511, pp. 502–510. Springer, Heidelberg (2012)
10. Mukhopadhyay, A., et al.: Morphological analysis of the left ventricular endocardial surface using a bag-of-features descriptor. *IEEE J-BHI* **19**(4), 1483–1493 (2014)
11. Ovsjanikov, M., et al.: Functional maps: a flexible representation of maps between shapes. *SIGGRAPH* **31**(4), 30 (2012)

12. Ovsjanikov, M., et al.: Analysis and visualization of maps between shapes. *CGF* **32**(6), 135–145 (2013)
13. Rustamov, R.M., et al.: Map-based exploration of intrinsic shape differences and variability. *ACM TOG* **32**(4), 72 (2013)
14. Wong, S.P., et al.: Relation of left ventricular sphericity to 10-year survival after acute myocardial infarction. *AJC* **94**(10), 1270–1275 (2004)
15. Peyre, G.: Toolbox Graph. <http://www.mathworks.com/matlabcentral/fileexchange/5355-toolbox-graph>